# MRI-Based 3D Shape Analysis of Thigh Muscles:

## *Patients with Chronic Obstructive Pulmonary Disease Versus Healthy Adults*

Bahareh HajGhanbari, BSc (PT), MSc, Ghassan Hamarneh, PhD, Neda Changizi, MSc, Aaron D. Ward, PhD, W. Darlene Reid, BMR (PT), PhD

**Rationale and Objective:** Because lower limb muscles differ in architecture and function, the systemic effects of chronic obstructive pulmonary disease (COPD) and related disuse may result in regional abnormalities. The purpose of this study was to investigate the differences between patients with COPD and healthy controls in three-dimensional shape and size measurements of individual thigh muscles.

**Materials and Methods:** Twenty patients with COPD and 20 healthy adults (aged 55–79 years) underwent magnetic resonance imaging of the thighs. After manual segmentation of individual knee extensor and flexor muscles, the three-dimensional shape of each muscle was obtained using specialized software. Eight shape descriptors were computed both globally (for the whole muscle) and regionally (for portions of the muscle). A two-tailed *t* test with a modified Bonferroni correction was used to compare group differences.

**Results:** Compared to the thigh muscles of healthy subjects, vastus intermedius and semimembranosus showed the most shape abnormalities in the COPD group ($P < .01$). Greater regional shape anomalies in the COPD group were found in the middle to proximal regions of all knee extensor muscles and the middle region of the semimembranosus muscle, compared to those of the control group ($P < .01$). In the COPD group, more shape abnormalities were found in the knee extensors than in the knee flexors ($P < .01$).

**Conclusions:** A non-uniform distribution of atrophy and size changes was found across knee extensors and flexors in patients with COPD. Further research is required to investigate the underlying mechanisms of regional morphologic abnormalities of the thigh muscles and the increased susceptibility of the knee extensors to atrophy-related anatomic anomalies in COPD.

**Key Words:** Thigh muscle; chronic obstructive pulmonary disease; magnetic resonance imaging; three-dimensional shape analysis; computer-aided diagnosis.



Skeletal muscle weakness, particularly in the lower extremities, is common in patients with chronic obstructive pulmonary disease (COPD) (1–3). In fact, lower limb muscles are typically more adversely affected than respiratory muscles in this patient population, in part because of disuse (3). COPD-related muscle weakness is also associated with other systemic comorbidities, including abnormal arterial blood gases (hypoxia, hypercapnia), malnutrition, systemic inflammation, oxidative stress, and low testosterone levels (2,4). Of interest, the magnitude of skeletal muscle weakness in patients with COPD ranges widely among patients (4), likely reflecting individual differences in the contribution of factors involved in poor muscle performance.

It has been suggested that the loss of muscle mass (size) is associated with skeletal muscle weakness in patients with COPD (3). However, the contribution of reduced muscle mass relative to other factors, such as changes in the muscle contractile apparatus and/or neuromuscular activation, is unknown (1). Comprehensive measures of muscle size and shape are therefore required to more precisely examine the relative contribution of muscle mass reduction to force loss. Magnetic resonance imaging (MRI) can be used to accurately distinguish muscle from bone, connective tissue, nerves, and blood vessels and can therefore provide accurate measures of muscle cross-sectional area (CSA) (5).

Achieving an accurate estimate of muscle size and atrophy is an important concern in strength training, aging, metabolic, and immobilization research (6), all of which aim to design effective preventive and therapeutic strategies. MRI can generate multiple image slices from which muscle volume can be estimated. Previous studies have used a single axial CSA as a surrogate measure of muscle size (3,7–11), and a few reports have described the measurement of several,

**Acad Radiol 2011;** 18:155–166

From the Department of Physical Therapy, University of British Columbia, Vancouver, BC V5Z 1M9, Canada (B.HG.); the Medical Image Analysis Lab, School of Computing Science, Simon Fraser University, Burnaby, BC, Canada (G.H., N.C.); the Robarts Research Institute, University of Western Ontario, London, ON, Canada (A.D.W.), and the Muscle Biophysics Laboratory, Vancouver Coastal Health Research Institute, Department of Physical Therapy, University of British Columbia, Vancouver, BC, Canada (W.D.R., B.HG.). Received June 23, 2010; accepted September 1, 2010. This study was supported by the Canadian Institutes of Health Research, the British Columbia Medical Services Foundation, and the British Columbia Lung Association. **Address correspondence to:** B.HG. e-mail: baharehg@interchange.ubc.ca


doi:10.1016/j.acra.2010.09.008

but not all, axial slices along the whole muscle (6,12). However, the measurement of CSA throughout all axial slices is preferable because it allows for a more accurate measure of muscle size (6). Of further concern, previous researchers have reported only on a single measure of thigh muscle CSA or the CSA of groups of thigh muscles (eg, knee extensors and flexors) rather than exploring individual thigh muscle volumes and size measures to determine whether aging and/or pathology differentially affect individual muscles (3,7–12).

Although muscle atrophy, as defined by muscle volume and CSA, has been reported in patients with COPD, other descriptors of surface area and shape abnormalities have not been explored (3,7,12). Three-dimensional (3D) shape descriptors can provide regional information about surface area, muscle size, and shape and the distribution of atrophy. However, whether muscle atrophy occurs uniformly or with intermuscle or intramuscle heterogeneity in COPD is unknown.

The objective of this study was to determine the differences between patients with COPD and healthy controls in 3D shape and size measurements of individual thigh muscles.

## MATERIALS AND METHODS

### Subjects

A convenience sample of patients with COPD was obtained from local hospitals and COPD clinics. Healthy older adults were recruited via advertisements in local newspapers and community centers. The inclusion criteria for patients with COPD were (1) moderate to severe (stage II to III) COPD on the basis of the Global Initiative for Chronic Obstructive Lung Disease guidelines (forced expiratory volume in 1 second < 80% of predicted value and forced expiratory volume in 1 second/forced vital capacity < 70%) (13) and (2) age > 50 years. The exclusion criteria for patients with COPD were no acute exacerbations and no oral corticosteroids during the 6 months prior to the study and no participation in a formal exercise rehabilitation program for ≥1 year prior to the study. The inclusion criteria for participants in the control group were age > 50 years, free of lung disease, nonsmokers, and no participation in any formal exercise rehabilitation program for ≥1 year prior to the study. The healthy group was matched for age, gender, and body mass index to facilitate the analysis of muscle shape and size independent of the overall size of the individual. As an additional normalization for patient size, we normalized the sizes of the muscles using the femur length as a surrogate measure of patient size. These individuals were screened for medical history and spirometric outcomes to ensure that no respiratory disease was present. The exclusion criteria for subjects in both groups included comorbid cardiovascular disease (eg, heart failure, previous myocardial infarction, or cardiovascular surgery), neurologic conditions (eg, stroke or Parkinson's disease), or lower-extremity musculoskeletal problems (eg, knee or hip injury or arthritis). All subjects provided written informed consent prior to participation in the study. Ethics approval was granted by the University Clinical Ethics Research Board at the University of British Columbia.

Height and weight were measured with shoes off and in light clothing. Spirometric measures were conducted according to the standards described by the American Thoracic Society (14) to measure forced expiratory volume in 1 second and forced vital capacity for the purposes of confirming the presence and severity of COPD. Descriptive demographic data of the participants are summarized in Table 1. Subjects were matched for gender and range matched for age and body mass index (ie, with the exception of a single outlier, no paired subjects had an age difference > 5 years or a body mass index difference > 4 kg/m$^2$).

### MRI

A 1.5T MRI scanner (1.5T Horizon Echospeed Scanner; GE Healthcare, Milwaukee, WI) was used to acquire 5 mm-thick, contiguous, axial slices from the anterior superior iliac spine to the tibial plateau while the subject's lower extremities were strapped to a foam block to minimize movement. Images were T1-weighted magnetic resonance (echo time, 8 ms; repetition time, 650 ms) with a 40 cm$^2$ field of view and a 512 × 384 pixel matrix (in-plane resolution, 0.78 × 1.78 mm). For each subject, two sets of images, one for the upper and another for the lower thigh regions, were collected in immediate succession without a change in the subject's position. A landmark (vitamin E capsule) at the midthigh (half the distance between the anterior inferior iliac spine and the superior margin of patella) was identified on the MRI scans to register the two images into a single image of the entire thigh. The vitamin E landmark facilitated the identification of overlap between the two sets of images. The MRI scan yielded a total of approximately 100 slices for each participant, which were merged into a single 3D image using the Merge module in the Amira 3.1 software package (Mercury Computer Systems, Inc, Chelmsford, MA), with the coincidence of the landmark verified after merging. Figure 1 shows a selection of representative MRI slices taken from a subject's thigh at different levels.

### Image Segmentation and Interpolation

ITK-SNAP 1.6.0.1 (15) was used for the manual slice-by-slice (5 mm slice thickness) segmentation of individual muscles from the merged axial magnetic resonance images (Fig 2). Segmentation was performed by a physical therapist with expert anatomic knowledge, which was further validated by cross-checking of several references (16–18) and educational inspection of human cadavers. Tendons and noncontractile tissue, including fascia, adipose tissue, and blood vessels outside the muscle periphery, were excluded. After the

**TABLE 1. Characteristics of Patients with COPD and Healthy Older Adults**

| Characteristic | Healthy Older Adults ($n$ = 20) | Patients with COPD ($n$ = 20) |
|---|---|---|
| Age (y) | 64.4 ± 8.1 | 68.2 ± 10.0 |
| Women/men | 11/9 | 11/9 |
| Height (m) | 1.67 ± 0.13 | 1.66 ± 0.09 |
| Weight (kg) | 69.0 ± 14.4 | 72.1 ± 14.6 |
| BMI (kg/m$^2$) | 24.3 ± 2.2 | 26.6 ± 4.7 |
| **Lung function** | | |
| $FEV_1$ (L) (% predicted)* | 2.28 ± 0.72 (81 ± 20) | 1.34 ± 0.41 (51 ± 17) |
| FVC (L) (% predicted)* | 3.05 ± 1.11 (83 ± 20) | 2.58 ± 0.47 (78 ± 14) |
| $FEV_1$/FVC (%)* | 77 ± 9 | 52 ± 14 |

BMI, body mass index; COPD, chronic obstructive pulmonary disease; $FEV_1$, forced expiratory volume in 1 second; FVC, forced vital capacity.
*Significant difference between groups at $P < .05$.

completion of slice-by-slice muscle segmentation, the muscle surfaces were interpolated in the out-of-plane direction using custom software in MATLAB version 7.6 (The MathWorks, Natick, MA) to obtain a rich description of the surface of each muscle (Fig 3). This interpolation was performed by establishing a correspondence between neighboring points on adjacent contours and then adding new surface points at equal (1 mm) distances along the line segments joining corresponding points. Muscle size was normalized to femur length as a surrogate measure of patient size by scaling the muscle surface point coordinates to the ratio of the patient's femur length to a reference femur length (mean of all observed femur lengths).

### Shape Descriptor Computation

We computed seven 3D shape and size descriptors of each of the muscles, described in the following paragraphs. All shape descriptors were computed globally, for each muscle as a whole. Four of the shape descriptors were computed regionally, whereby each muscle was divided into four quarters (regions) along its length (Fig 4), and the measures were calculated for each region.

*Mean Distance to the Centroid (MDC) and Standard Deviation of Distances to the Centroid (SDC).* The centroid of a 3D shape is a point in three dimensions that is in the center of the shape. Intuitively, it can be thought of as a point that is not biased toward any region or side of the shape over another. The distances from each point on the shape surface to this centroid can be analyzed to obtain two measures: (1) the overall size of the object (by taking the mean) and (2) the difference between the shape and a perfect sphere (by taking the standard deviation). For a perfectly spherical shape, these distances will all be the same, and their mean (the MDC) will be exactly equal to the radius of the sphere. As the shape becomes less spherical, these distances become more different from one another; this is reflected in their standard deviation (the SDC). Figure 5 illustrates how the magnitude of the SDC reflects asphericity in the form of surface roughness or irregularity. These measures were computed regionally by averaging the MDC and SDC values computed for each slice within each region.

*Three-dimensional Moment Invariants.* Three 3D moments, $J_1$, $J_2$, and $J_3$, which are invariant to translation and rotation, were computed for the surface points of each muscle. Intuitively, moments capture characteristics of the spatial distribution of the voxels that make up the muscle surface (19). Informally, these are considered to be higher order extensions of quantities such as the mean and standard deviation. The moment invariants were calculated using the methodology described by Ward et al (20).

Moment invariants could not be assessed regionally, because the division of the muscle introduces sudden flat caps at the division boundaries, which would result in misleading moment measurements.

*Surface Area and Volume.* To compute the surface area of each muscle, the closest points on the contours of adjacent slices were connected to form a triangular mesh (Fig 6). The sum of the triangular areas provided an estimate of muscle surface area (21). The volume of each muscle was computed by counting the number of voxels inside the segmentation of the muscle and multiplying this number by the spatial volume occupied by each voxel. This measure was also computed regionally.

### Statistical Analysis

Comparisons of muscle shape and size measures were performed using SPSS version 16.0 (SPSS, Inc, Chicago, IL). Each descriptor was tested for normality using the Shapiro-Wilk test, which showed that the data were normally distributed ($P > .05$). As such, a two-tailed $t$ test was performed for each descriptor to evaluate the null hypothesis, which stated that the means of the healthy and COPD groups did not differ. For the regional analysis, the $t$ test was repeated for three regional features because of removal of extreme outlier values (outliers were defined as ±2 standard deviations or more). The $P$ values reported by the $t$ tests indicated the statistical significance of the differences in the measurements

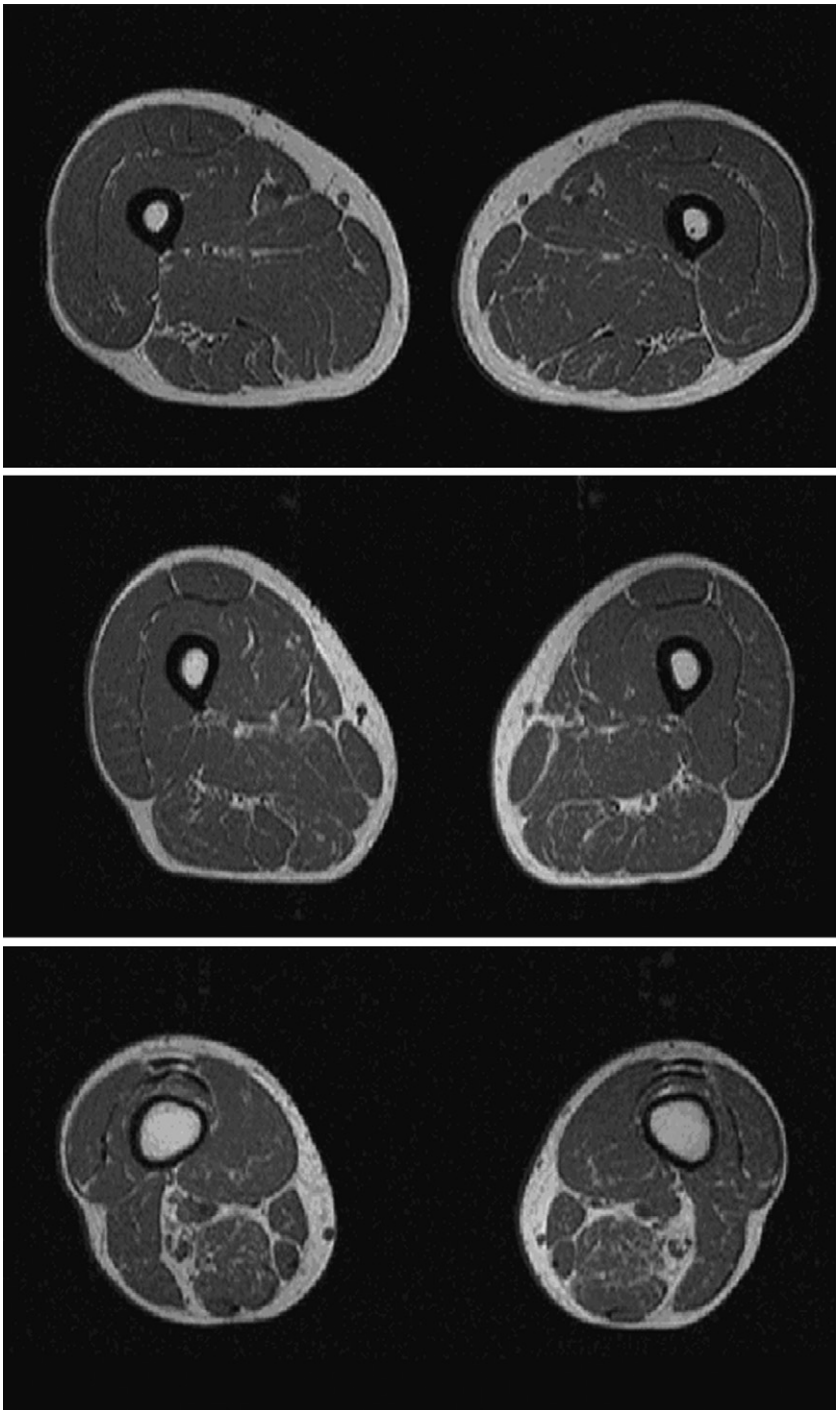

**Figure 1.** Sample MRI slices of a subject's thigh from proximal (top) to distal (bottom).

in the COPD group compared to the healthy control group. Because the outcomes (shape features) were highly correlated (with the pairwise correlation within each of two groups for each shape descriptor lying within the range of 0.8 to 0.9), a Bonferroni correction seemed to be an overly conservative approach (22). Therefore, we applied a modified Bonferroni correction to avoid potential type I error for multiple comparisons (22). The preestablished level of significance of $\alpha = .01$ was selected for the comparison of shape descriptors for global and regional analyses. The null hypothesis was rejected for measurements which resulted in $P$ values $< \alpha$ and therefore were considered to be statistically significant (Table 2).

### *Classification Accuracy*

The shape measures from global analysis were compared to test their clinical significance by evaluating the ability of a trained automated classifier to distinguish the healthy from the COPD groups using the computed measures. We input the entire feature vector of each muscle into a soft-margin

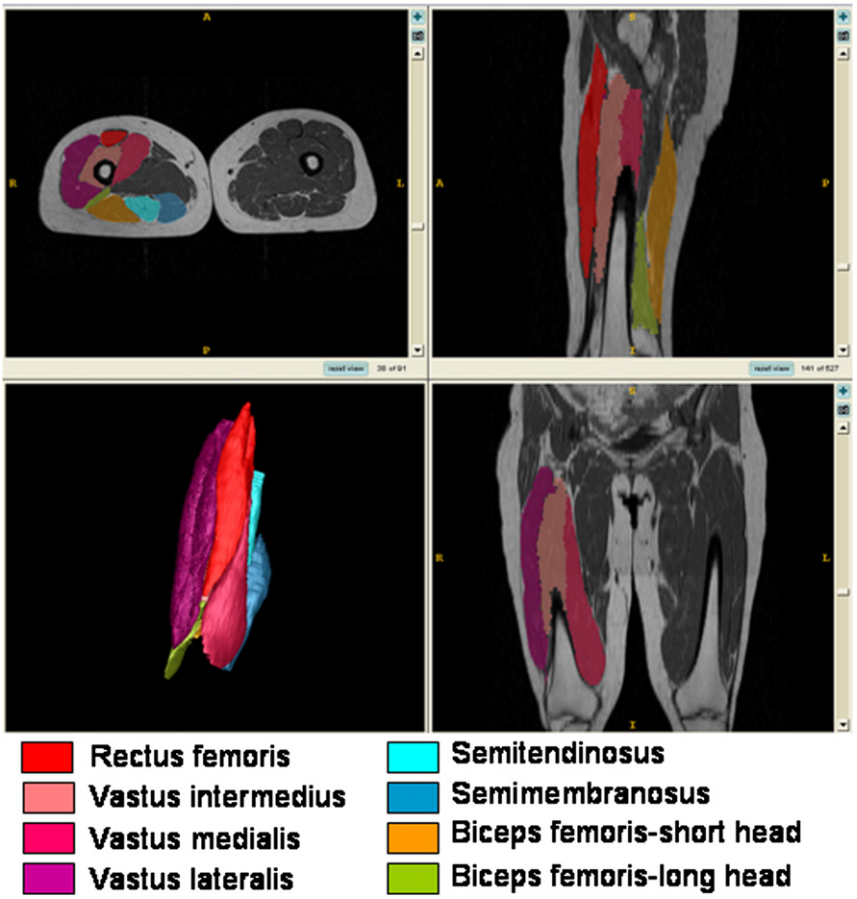


**Figure 2.** Sample segmentation of knee extensor and flexor muscles in ITK-SNAP: axial (top left), sagittal (top right), coronal (bottom right), and 3D mesh view (bottom left). The different knee extensors and flexors are represented by different fill colors.

nonlinear support vector machine (SVM) classifier (23). The SVM classifier classifies subjects as normal or COPD on the basis of a chosen feature vector. We chose to consider all of the features together rather than each feature individually to improve the discrimination between the two groups (the differences between which are given in Table 1). We then measured the classification accuracy as the percentage of correct classifications reported in a leave-one-out cross-validation.

## RESULTS

### *Analysis of Global Muscle Shape Descriptors*

The results of the analysis of the global shape descriptors of the knee extensor and the knee flexor muscles are presented in Table 2, which shows the six measures of the five muscles for which statistically significant differences were found between the normal and the COPD groups. In general, all of the values for the seven shape descriptors were smaller in the COPD group compared to the healthy controls. Knee extensors showed more shape abnormalities in the COPD group compared to healthy controls ($P < .01$). Of the knee extensors, the vastus intermedius showed significant differences in seven shape descriptors in the COPD group compared to healthy subjects. The box plots in Figure 7 depict the sampling distribution of global shape descriptors of the vastus intermedius. The vastus medialis and rectus femoris showed significant differences in one (surface area) and two (moments 1 and 2) shape descriptors, respectively, in the COPD group compared to healthy subjects. Fewer shape abnormalities were found in the knee flexors compared to the knee extensors. Of the knee flexors, significant shape abnormalities were found in the semimembranosus in MDC, SDC, and moment 1. The short head of the biceps femoris showed significantly lower values in moments 1 and 2 (which reflect differences in the distribution of muscle mass) in patients with COPD. In general, among all of the knee flexor and extensor muscles, shape abnormalities were most apparent in the semimembranosus and vastus intermedius muscles of patients with COPD. The semitendinosus, the long head of biceps femoris and vastus lateralis did not show any differences in shape descriptors. Although muscle volumes in patients with COPD were lower, no significant differences in volumes of any of the knee extensor and flexors were found between groups.

### *Analysis of Regional Muscle Shape Descriptors*

The regional morphology of knee extensor and flexor muscles was then investigated more closely by examining each muscle in four regions, subdivided into four equal distances along the total length of each muscle from origin to insertion (Fig 4).

Significant results related to the regional analysis of 3D shape descriptors, including *P* values, are presented in Table

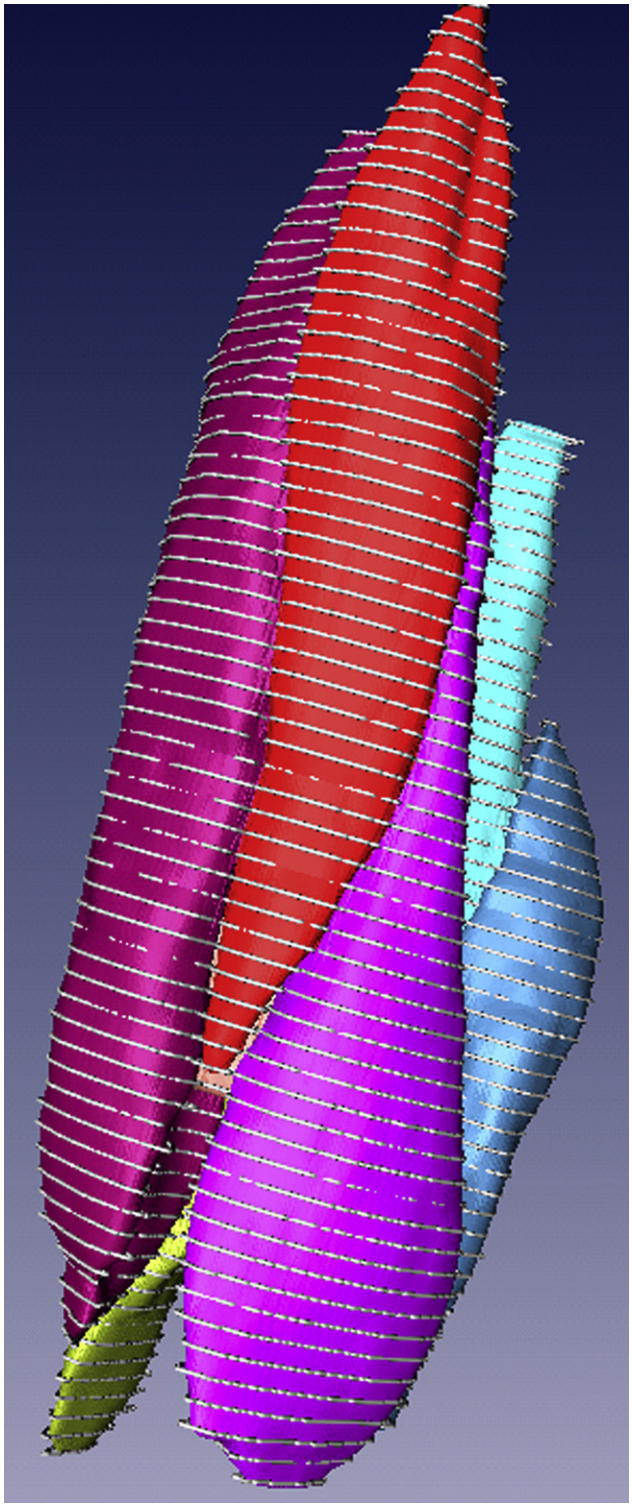

**Figure 3.** The interpolation technique for knee extensor and flexor muscles. The parallel white contours depict the segmentation boundaries on the acquired magnetic resonance slices with a 5-mm interslice spacing. The colored regions uniting the segmentation boundaries are the product of the interpolation technique.

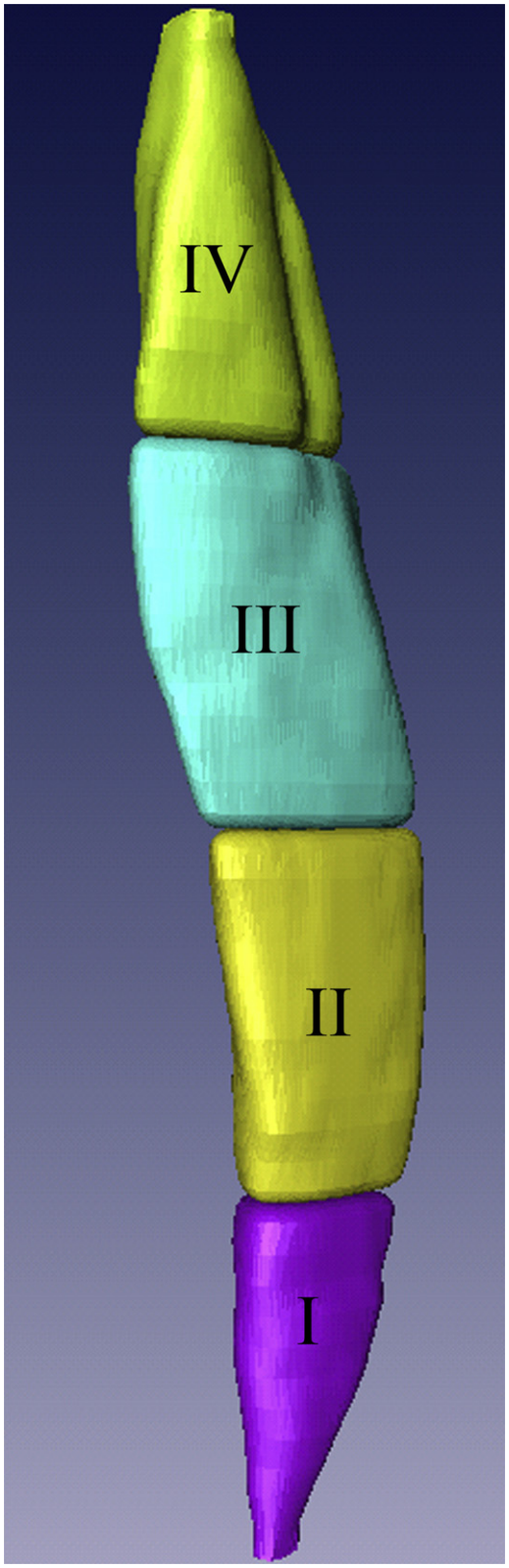


**Figure 4.** A sample muscle (rectus femoris) divided into four regions (quarters) as defined by four equal lengths along the vertical axis of the muscle. Region IV is most proximal, whereas region I is the most distal.

3. In the COPD group, knee extensors showed significantly lower measures in shape descriptors (ie, more shape abnormalities) in the middle to proximal regions of the muscles, whereas shape abnormalities in the knee flexors were found closer to the insertion of the muscles (ie, distal sections).

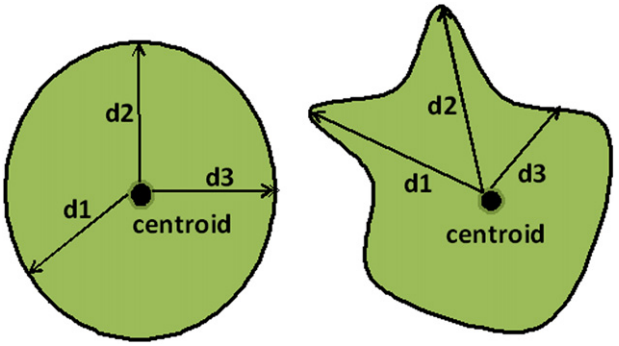


**Figure 5.** Description of the standard deviation of distances to centroid (SDC) measure. Three such distances are illustrated as d1, d2, and d3. Note how a perfect circle or sphere exhibits zero variability in the distances to the centroid (left), whereas the standard deviation of these differences will not be zero for a rough or irregular shape with more variability in d1, d2, and d3 (right).

Among the knee extensors, the vastus medialis showed the highest number of regional abnormalities in the COPD group, whereas the vastus lateralis, rectus femoris, and vastus intermedius showed lower numbers of regional shape abnormalities. SDC, an indicator of surface roughness, was significantly lower in the COPD group in region III of the rectus femoris and regions II, III, and IV of the vastus medialis. Surface area was significantly lower in the COPD group in regions II and III of the vastus medialis and region III of the vastus lateralis and rectus femoris. Significantly lower volumes were found in regions II and III of the vastus lateralis in the COPD group. Of the knee flexors, regional shape abnormalities were mainly found in the distal regions of semimembranosus (ie, area and volume of region II). No significant differences between groups were found when the short and long heads of the biceps femoris and semitendinosus were examined for regional differences.

### *Classification Accuracy*

The SVM classifier provided 95% to 100% accuracy in differentiating muscles from healthy subjects from those of patients with COPD (Table 4). Our implementation requires two parameters: one assigning a penalty $C$ to classification errors and another defining the width $\gamma$ of a radial basis function used within the SVM. A standard logarithmic grid search was used to determine the optimal values for the parameters $C$ and $\gamma$ for each muscle type using leave-one-out cross-validation.

## DISCUSSION

### *Differences in MDC, Surface Area, and SDC*

Higher MDC and surface area values in healthy group reflect a bigger muscle girth. However, one intuitively expects that measures of size, including MDC, surface area, and volume of the muscle, should all increase as the size of the muscle increases. In this study, we observed increases in MDC and surface area in

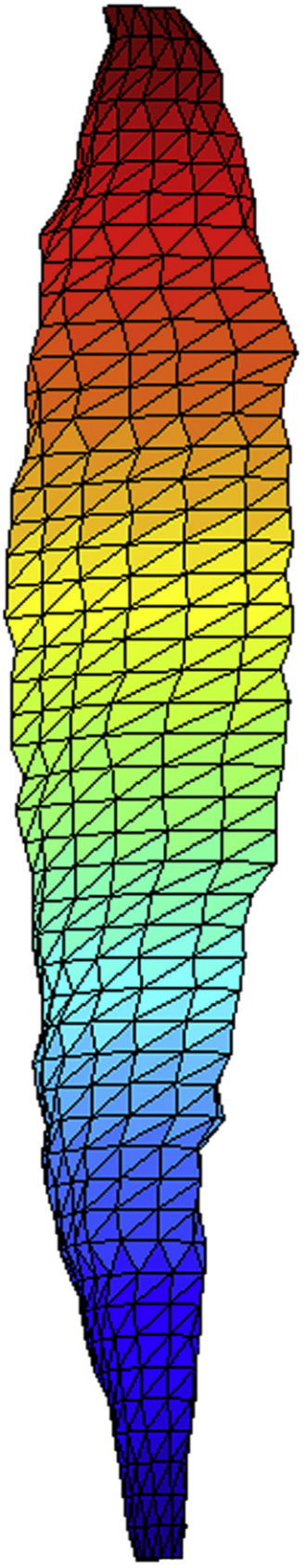

**Figure 6.** A triangular mesh represents the muscle surface area. The surface area of the muscle is estimated as the sum of the area of all triangles that constitute the mesh.

**TABLE 2. Differences Between 3D Shape Descriptors for Global Analysis in Healthy Subjects Compared to Patients with COPD**

| Muscle | MDC (mm) | SDC (mm) | Moment 1 ($mm^2$) | Moment 2 ($mm^4$) | Moment 3 ($mm^6$) | Area ($mm^2$) |
|---|---|---|---|---|---|---|
| RF | | | | | | |
| Mean (SE) | 3.08 (1.33) | 1.19 (0.74) | 7.68E7 (2.91E7)* | 4.78E15 (1.71E15)† | 4.18E22 (1.84E22) | 2,549.10 (1,523.03) |
| 95% CI | 0.39–5.79 | 0.31–2.70 | 1.78E7–1.36E8 | 1.32E15–8.25E15 | 4.58E21–7.91E22 | 534.11–5,632.31 |
| VI | | | | | | |
| Mean (SE) | 5.31 (1.66)† | 3.12 (1.00)† | 1.58 E8 (5.52E7)† | 1.83E16 (6.42E15)† | 4.87E23 (1.81E23)* | 7,492.95 (2,364.59)† |
| 95% CI | 1.95–8.67 | 1.08–5.15 | 4.57E7–2.69E8 | 5.31E15–3.13E16 | 1.22E23–8.52E23 | 2,706.08–12,279.82 |
| VM | | | | | | |
| Mean (SE) | 2.12 (1.06) | 0.74 (0.79) | 8.49E7 (4.15E7) | 1.11E16 (5.33E15) | 2.83E23 (1.46E23) | 4,667.11 (1,770.98)* |
| 95% CI | 0.03–4.27 | 0.87–2.35 | 9.07E5–1.69E8 | 3.14E14–2.19E16 | 1.14E22–5.78E23 | 1,081.94–8,252.27 |
| BF-SH | | | | | | |
| Mean (SE) | 3.78 (1.55) | 2.13 (0.855) | 3.65E7 (1.39E7)* | 7.15 E14 (2.71E14)* | 2.84 E21 (1.21E21) | 2,277.42 (1,171.59) |
| 95% CI | 0.63–6.92 | 0.40–3.87 | 8.39E6–6.47E7 | 1.68E14–1.26E15 | 3.96E20–5.29E21 | 94.35–4,649.18 |
| SM | | | | | | |
| Mean (SE) | 5.30 (1.56)† | 2.47 (0.88)† | 7.49E7 (2.36E7)† | 3.25E15 (1.46E15) | 3.87E22 (1.97E22) | 4,516.24 (1,732.28)* |
| 95% CI | 2.15–8.45 | 0.689–4.24 | 2.71E7–1.23E8 | 2.99E14–6.21E15 | 1.21E21–7.86E22 | 1,009.41–8,023.07 |

Statistical measures are reported as mean difference (SE) and 95% CI of the difference. Mean difference is defined as the average absolute difference of group means for each shape descriptor (independent values).

BF-SH, biceps femoris–short head; CI, confidence interval; COPD, chronic obstructive pulmonary disease; MDC, mean distance to the centroid; RF, rectus femoris; SDC, standard deviation of distances to the centroid; SE, standard error; SM, semimembranosus; VI, vastus intermedius; VM, vastus medialis.

*Significant difference between groups at $P < .01$.

†Significant difference between groups at $P < .005$.

the normal group, without a concomitant increase in muscle volume. To understand these results, it is important to note that these three measures are different in the way they describe the muscle size, and the term "muscle size" can imply different meanings. For example, the "size" of a sphere increases as its volume, surface area, or MDC (or radius) increases. However, these three measures relate differently to the radius $r$ of the sphere; volume is proportional to $r^3$, surface area is proportional to $r^2$, and MDC is proportional to $r$, and so they all relate to "size" in different ways. Some size measures are more sensitive to changes in the radius or thickness of the muscle than others. For example, if the radius doubles, the volume will increase by an approximate factor of 8, whereas the surface area only increases by an approximate factor of 4.

The SDC measure reflects the variability in the thickness (or radius) of the entire muscle, or portions thereof, in global and regional analysis respectively. The closer SDC is to zero, the more constant the thickness of the muscle and the more closely the muscle approximates a sphere shape with a fixed radius from the center to any point on the surface. As such, the significant increase in SDC alone indicates that regardless of differences in volume, the thickness differs along the muscle or muscle section. Likewise, the lower SDC indicates fewer indentations on the surface and smoother muscle periphery.

### *Physiologic Implications of Global and Regional Measurements*

Our results indicated that the semimembranosus and vastus intermedius had smaller or fewer indentations or folds (lower SDC) at their periphery in the COPD group. Three possible reasons might explain this lower surface irregularity in patients with COPD. First, in the elderly, fascicles within the muscle become shorter and less pennate (24,25), mainly because of decreases in the contractile tissue packed along the tendon aponeurosis (24). Second, this phenomenon becomes even more apparent in cases of disuse (26). Because knee extensors are primarily pennate muscles (27), it is likely that they are more susceptible to the pennation-reducing effects of disuse in COPD, resulting in a reduction in the indentation of the muscle surface. Third, the selective atrophy of type II fibers in COPD (28), which are more superficially distributed in the quadriceps (29), might also contribute to the reduced surface irregularity.

Moreover, lower regional surface area and SDC were detected, while muscle volumes were only nonsignificantly lower in patients with COPD. This might be related to age-related and disuse-related reductions in pennation angle and atrophy of superficial type II fibers of knee extensors in the COPD group, as discussed above. Other contributing factors to the loss of regional surface irregularity could include regional neuropathic changes with associated motoneuron death and/or muscle cell apoptosis, which would lead to a marked decrease in the number as well as the size of muscle fibers. Previous studies provide evidence in support of polyneuropathy (30,31) and skeletal muscle myopathy (30) due to local increases in cytokines and reactive oxygen species within the muscle as well as corticosteroid use (32) in COPD.

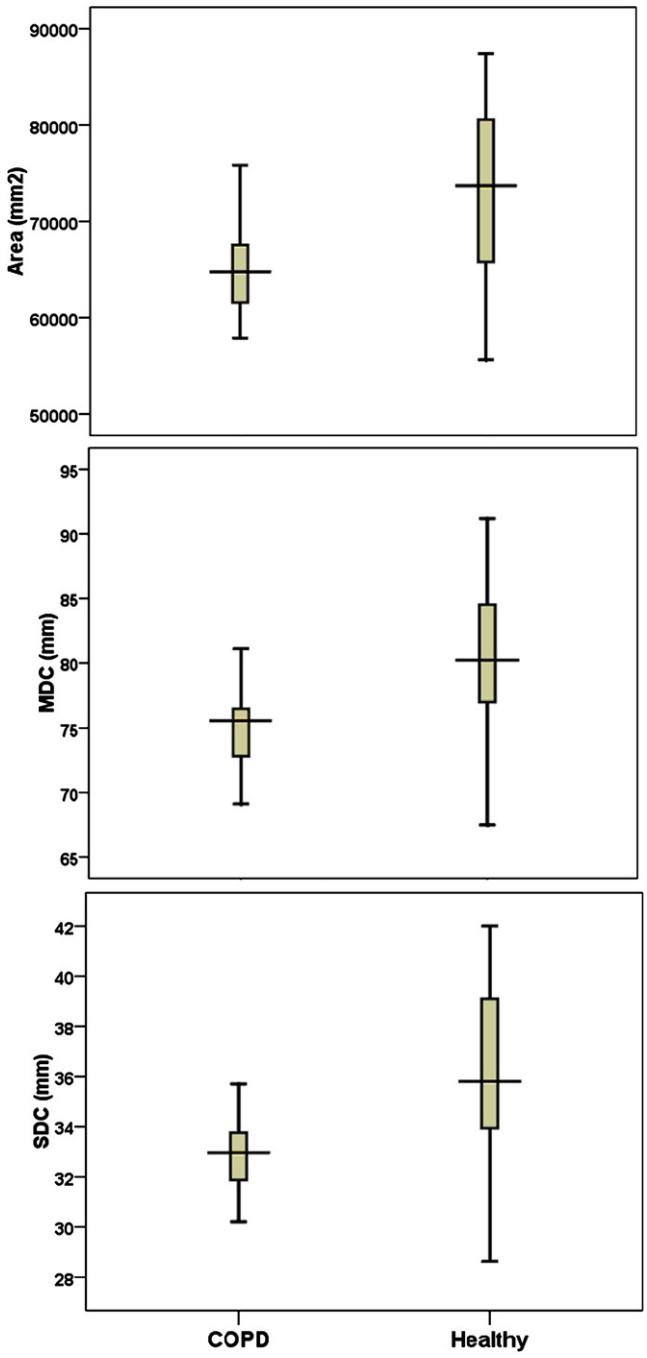


**Figure 7.** Sampling distribution of surface area (top), mean distance to the centroid (MDC; middle), and standard deviation of distances to the centroid (SDC; bottom) for the vastus intermedius. COPD, chronic obstructive pulmonary disease.

### *Distribution of Shape Abnormalities and Atrophy Among Thigh Muscles in COPD*

In the regional analysis, most differences between groups were found in the middle two regions, not regions I (distal) or IV (proximal), of the muscles. This could be related to the fact that thigh muscles taper closer to their origins and insertions such that less muscle mass is present in the end regions.

Furthermore, although shape abnormalities were present throughout the middle to proximal regions of the knee extensor, morphologic anomalies were less evident among knee flexors and were mainly restricted to the distal regions closer to the insertion of the muscles (ie, region II of the semimembranosus). Significant atrophy of the middle two regions of the vastus lateralis and region II of the semimembranosus was evidenced by the reductions in volume and surface area of these sections in the COPD group. The differential patterns of shape abnormalities between knee extensors and flexors require further study. One possibility is that this variability could be related to the increased muscle fat infiltration (12,33), neuropathy, and polyneuropathy (30,31) that are characteristic of COPD. In line with this, selective pathology of femoral or tibial nerves or branches, or regional loss of motor neurons, might be involved in the regional atrophy of these muscles.

### *Measurement of Muscle Volume and Comparison to Previous Studies*

We found no significant differences in muscle volumes between the two groups in our global analysis, although values tended to be lower in patients with COPD. Our results are discordant with those of previous studies that described lower muscle volumes in patients with COPD compared to healthy controls (3,7,12). This discrepancy might be due to different methodologies used to estimate muscle size. Previous studies reported on muscle groups (3,12), rather than individual thigh muscles, which may have masked and diminished variances in regional muscle atrophy. A second issue is the small sample sizes and locations of the thigh muscle slices used to estimate volume in previous studies. A single CSA (3,7) at the midthigh or the CSA of a number of slices (12) was used to estimate thigh muscle mass in these studies. Midthigh measures may represent the largest differences between healthy subjects and those with COPD, so a single slice at the midthigh may exaggerate differences between COPD and healthy subjects. Even when using multiple slices (12), muscle volumes were calculated by summing 17 selected slices plus estimated volumes of intermediate sections on the basis of the truncated cone formula. This technique is based on the tenuous assumption that the muscle is conical in shape, which may not accurately reflect thigh muscle shapes (6,34).

### *Automated Group Classification on the Basis of Shape Measures*

The trained SVM-based classifier is capable of distinguishing between the COPD and healthy groups with an accuracy of 95% to 100% across the eight thigh muscles examined. Although it was not our objective to immediately develop a computer-aided diagnosis system for individual thigh muscles, the accuracy of these classifications provide support for future work to translate this technique to the clinic.

**TABLE 3. Differences of Three-dimensional Shape Descriptors for Regional Analysis in Healthy Subjects Compared to Patients with COPD**

| Muscle | Shape Descriptor | Region* | Mean (SE) of Difference | *P* | 95% CI of Difference |
|---|---|---|---|---|---|
| RF | SDC (mm) | III | 0.91(0.32) | .004 | 0.26–1.54 |
| | Area ($mm^2$) | III | 1,280.20 (460.65) | .008 | 347.66–2,212.73 |
| VL | Volume ($mm^3$) | II | 35,101.15 (9,491.81) | .001 | 15,850.87–54,351.44 |
| | Volume ($mm^3$) | III | 31,114.11 (8,840.89) | .001 | 13,200.76–49,027.46 |
| | Area ($mm^2$) | III | 2,373.28 (860.72) | .009 | 629.30–4,117.26 |
| VI | Area ($mm^2$) | III | 2,634.61 (739.64) | .001 | 1,137.29–4,131.94 |
| VM | SDC (mm) | II | 0.87 (0.26) | .001 | 0.35–1.39 |
| | SDC (mm) | III | 1.28 (0.33) | .000 | 0.62–1.94 |
| | SDC (mm) | IV | 0.96 (0.29) | .002 | 0.37–1.56 |
| | Area ($mm^2$) | II | 1,461.19 (475.00) | .004 | 499.60–2,422.79 |
| | Area ($mm^2$) | III | 1,160.76 (313.56) | .001 | 523.54–1,797.99 |
| SM | Area ($mm^2$) | II | 1,441.56 (546.37) | .005 | 335.48–2,547.64 |
| | Volume ($mm^3$) | II | 16,631.14 (5,140.63) | .003 | 6,215.23–27,047.05 |

The shape descriptors and corresponding regions that revealed significant between group differences in regional analysis are presented in columns 2 and 3, respectively. Statistical measures are reported as mean difference (SE) and 95% CI of the difference. Mean difference is defined as the average absolute difference of group means for each shape descriptor (independent values).

CI, confidence interval; COPD, chronic obstructive pulmonary disease; RF, rectus femoris; SDC, standard deviation of distances to the centroid; SE, standard error; SM, semimembranosus; VI, vastus intermedius; VL, vastus lateralis; VM, vastus medialis.

*Regions are defined in the text and Figure 6.

**TABLE 4. SVM Classification Rates**

| Muscle Groups | Muscle | Classification Rate Using All Features (%) |
|---|---|---|
| Knee extensors (quadriceps) | Rectus femoris | 99.9 |
| | Vastus medialis | 97.0 |
| | Vastus intermedius | 99.9 |
| | Vastus lateralis | 97.5 |
| Knee flexors (hamstrings) | Biceps femoris–long head | 99.9 |
| | Biceps femoris–short head | 95.0 |
| | Semimembranosus | 97.3 |
| | Semitendinosus | 99.8 |

SVM, support vector machine.

### *Significance of the Study*

This is the first study to examine 3D shape analysis and the distribution of atrophy among thigh muscles in patients with COPD. The main differences between our study and previous investigations are as follows: (1) we used a 3D approach that takes measurements throughout the volume of the muscle, (2) we computed a rich set of shape measurements augmenting the typical CSA measure used in this domain, and (3) we performed a regional analysis to quantify any differential changes in shape and volume that are consequent to COPD. CSA and muscle volume have been previously used as the only estimates of muscle mass and size. Our study suggests that these two measures provide an incomplete estimate of the overall size of the muscle and thus might not be sufficient to demonstrate the distribution of atrophy among thigh muscles in patients with chronic musculoskeletal conditions such as COPD. More comprehensive measures such as shape descriptors are required to understand the underlying pathologies that govern the loss of muscle mass in musculoskeletal conditions. Our study further suggests that atrophy-related shape changes might selectively target specific muscles or parts of a muscle, which requires further investigation.

### *Limitations and Future Work*

We acknowledge that a small sample size is a limitation of our study. However, the results of this study provide further impetus to investigate the etiology of regional muscle atrophy and shape abnormalities in COPD. Future work, using a larger sample size and parallel measurements of shape descriptors, regional muscle biopsy, angle of pennation, strength, and muscle fat infiltration, will be necessary to elucidate the mechanisms that govern not only the muscle atrophy characteristic of COPD but also the increased susceptibility of the

muscles of the anterior thigh to atrophy-related anatomic anomalies. The presence of muscle weakness in patients with COPD is well established. However, it is unclear whether it is secondary to loss of muscle mass or rather to deficits in muscle contractile function, fiber type distribution, neuromuscular activation, or some combination thereof. A better understanding of the pattern and etiology of COPD-related muscle atrophy and morphologic abnormalities would aid in the design of rehabilitative strategies for the purpose of improving age-related loss of muscle mass (sarcopenia) and physical disability among this population.

Future work is also motivated by the results given by the 3D moment invariant measures, which showed significant differences between the healthy and COPD groups. These measures could potentially be useful to the eventual computer-aided diagnosis of muscle abnormalities consequent to COPD or other disorders that affect muscle. Their efficacy in group differentiation also motivates future research exploring the utility of fine-scale, intuitive, localized shape representations, such as M-reps (35) and medial patches (36).

## CONCLUSIONS

Our study reveals that among the thigh muscles, morphologic changes appear more in knee extensor muscles than in knee flexors in patients with COPD. Furthermore, shape differences are most apparent in the middle to proximal regions of the knee extensors and the lower regions of the knee flexors in patients with COPD. These findings could inform the design of strength training programs as well as targeted prescription of therapeutics, such as neuromuscular electrical stimulation and biofeedback, to the more affected muscles or muscle sections. Our study suggests a need for more attention to the middle to proximal regions of the knee extensors (regions showing more atrophy or shape abnormalities). Furthermore, hypertrophied muscle is reported to have a higher angle of pennation compared with untrained muscle (26). Therefore, it is likely that a more appropriately localized treatment approach could improve the pennation angle in affected muscle regions in COPD.

## REFERENCES


1. Gosselink R, Troosters T, Decramer M. Peripheral muscle weakness contributes to exercise limitation in COPD. Am J Respir Crit Care Med 1996; 153:976–980.
2. Nici L, Donner C, Wouters E, et al. American Thoracic Society/European Respiratory Society statement on pulmonary rehabilitation. Am J Respir Crit Care Med 2006; 173:1390–1413.
3. Bernard S, LeBlanc P, Whittom F, et al. Peripheral muscle weakness in patients with chronic obstructive pulmonary disease. Am J Respir Crit Care Med 1998; 158:629–634.
4. Casaburi R. Skeletal muscle dysfunction in chronic obstructive pulmonary disease. Med Sci Sports Exerc 2001; 33:S662–S670.
5. Engstrom CM, Loeb GE, Reid JG, et al. Morphometry of the human thigh muscles: a comparison between anatomical sections and computer tomographic and magnetic resonance images. J Anat 1991; 176: 139–156.
6. Tracy BL, Ivey FM, Metter JE, et al. A more efficient magnetic resonance imaging-based strategy for measuring quadriceps muscle volume. Med Sci Sports Exerc 2003; 35:425–433.
7. Seymour JM, Ward K, Sidhu PS, et al. Ultrasound measurement of rectus femoris cross-sectional area and the relationship with quadriceps strength in COPD. Thorax 2009; 64:418–423.
8. Marquis K, Debigare R, Lacasse Y, et al. Midthigh muscle cross-sectional area is a better predictor of mortality than body mass index in patients with chronic obstructive pulmonary disease. Am J Respir Crit Care Med 2002; 166:809–813.
9. Akima H, Kano Y, Enomoto Y, et al. Muscle function in 164 men and women aged 20-84 yr. Med Sci Sports Exerc 2001; 33:220–226.
10. Visser M, Goodpaster BH, Kritchevsky SB, et al. Muscle mass, muscle strength, and muscle fat infiltration as predictors of incident mobility limitations in well-functioning older persons. J Gerontol A Biol Sci Med Sci 2005; 60:324–333.
11. Overend TJ, Cunningham DA, Kramer JF, et al. Knee extensor and knee flexor strength: cross-sectional area ratios in young and elderly men. J Gerontol 1992; 47:M204–M210.
12. Mathur S, Takai KP, Macintyre DL, et al. Estimation of thigh muscle mass with magnetic resonance imaging in older adults and people with chronic obstructive pulmonary disease. Phys Ther 2008; 88:219–230.
13. Global Initiative for Obstructive Lung Disease. Global strategy for the diagnosis, management and prevention of chronic obstructive pulmonary disease. Bethesda, MD: National Heart, Lung and Blood Institute, 2004. 6–8.
14. American Thoracic Society/European Respiratory Society. Skeletal muscle dysfunction in chronic obstructive pulmonary disease: a statement of the American Thoracic Society and the European Respiratory Society. Am J Respir Crit Care Med 1999; 159:S1–S40.
15. Yushkevich PA, Piven J, Hazlett HC, et al. User-guided 3D active contour segmentation of anatomical structures: significantly improved efficiency and reliability. Neuroimage 2006; 31:1116–1128.
16. Agur AMR, Grant JCB, Dalley AF. Grant's atlas of anatomy. 12th ed. Philadelphia: Lippincott Williams & Wilkins, 2009.
17. Marinkovic S, Schellinger D, Milisavljevic M, et al. Sectional and MRI anatomy of the human body: a photographic atlas. Stuttgart, Germany: Thieme Verlag, 2000.
18. Willan PLT, Ransome JA, Mahon M. Variability in human quadriceps muscles: Quantitative study and review of clinical literature. Clin Anat 2002; 15:116–128.
19. Sadjadi FA, Hall EL. Three dimensional moment invariants. IEEE PAMI 1980; 2:127–136.
20. Ward AD, Hamarneh G, Ashry R, et al. 3D shape analysis of the supraspinatus muscle: a clinical study of the relationship between shape and pathology. Acad Radiol 2007; 14:1229–1241.
21. Lorensen WE, Cline HE. Marching cubes: a high resolution 3D surface construction algorithm. Comput Graph 1987; 21:163–169.
22. Pocock SJ, Geller NL, Tsiatis AA. The analysis of multiple endpoints in clinical trials. Biometrics 1987; 43:487–498.
23. Fradkin D, Muchnik I. Support vector machines for classification. DIMACS Ser Discrete Math Theoret Comput Sci 2006; 70:13–20.
24. Narici MV, Capodaglio P. Changes in muscle size and architecture in disuse-atrophy. In: Capodaglio P, Narici MV, eds. Muscle atrophy: disuse and disease. Pavia, Italy: PI-ME Press, 1998; 55–63.
25. Kubo K, Kanehisa H, Azuma K, et al. Muscle architectural characteristics in young and elderly men and women. Int J Sports Med 2003; 24:125–130.
26. Kawakami Y, Abe T, Fukunaga T. Muscle-fiber pennation angles are greater in hypertrophied than in normal muscles. J Appl Physiol 1993; 74:2740–2744.
27. Kendall FP, McCreary EK, Provance PG, et al. Muscles: testing and function with posture and pain. 5th ed. Baltimore, MD: Lippincott Williams & Wilkins, 2005.
28. Gosker HR, Engelen MP, van Mameren H, et al. Muscle fiber type IIX atrophy is involved in the loss of fat-free mass in chronic obstructive pulmonary disease. Am J Clin Nutr 2002; 76:113–119.
29. Johnson MA, Polgar J, Weightman D, et al. Data on the distribution of fibre types in thirty-six human muscles: an autopsy study. J Neurol Sci 1973; 18: 111–129.
30. Faden A, Mendoza E, Flynn F. Subclinical neuropathy associated with chronic obstructive pulmonary disease: possible pathophysiologic role of smoking. Arch Neurol 1981; 38:639–642.
31. Pozza JJ, Marti-Masso JF. Peripheral neuropathy associated with chronic obstructive pulmonary disease. Neurologia 1997; 12:12389–12394.
32. Agusti AGN, Noguera A, Sauleda J, et al. Systemic effects of chronic obstructive pulmonary disease. Eur Respir J 2003; 21:347–360.

33. Mathur S, MacIntyre DL, Forster BB, et al. Fat infiltration in the quadriceps and hamstrings in people with COPD and lung transplant recipients. Med Sci Sports Exerc 2005; 37:S243–S244.
34. Roberts N, Cruz-Orive LM, Reid MK, et al. Unbiased estimation of human body composition by the cavalieri method using magnetic resonance imaging. J Microsc 1993; 171:239–253.
35. Pizer SM, Fletcher PT, Joshi S, et al. Deformable M-reps for 3D medical image segmentation. Int J Comput Vis 2003; 55:85–106.
36. Hamarneh G, Ward AD, Frank R. Quantification and visualization of localized and intuitive shape variability using a novel medial-based shape representation. Proc IEEE Conf Int Symp Biomed Imaging 2007; 1232–1235.